HHS Public Access

Author manuscript

Oncogene. Author manuscript; available in PMC 2014 October 17.

Published in final edited form as:

Oncogene. 2014 April 17; 33(16): 2110–2122. doi:10.1038/onc.2013.160.

Tumor-derived mural-like cells coordinate with endothelial cells: role of YKL-40 in mural cell-mediated angiogenesis

Ralph Francescone[1], **Nipaporn Ngernyuang**[2], **Wei Yan**[3], **Brooke Bentley**[3], and **Rong Shao**[1,3,4,*]

[1]Molecular and Cellular Biology Program, Morrill Science Center, University of Massachusetts, Amherst, MA 01003

[2]Graduate School, Khon Khaen University, Khon Khaen, Thailand, 40002

[3]Pioneer Valley Life Sciences Institute, 3601 Main Street, Springfield, MA 01199

[4]Department of Veterinary and Animal Sciences, University of Massachusetts, Amherst, MA 01003

Abstract

Tumor neo-vasculature is characterized by spatial coordination of endothelial cells with mural cells, which delivers oxygen and nutrients. Here, we explored a key role of the secreted glycoprotein YKL-40, a mesenchymal marker, in the interaction between endothelial cells and mesenchymal mural-like cells for tumor angiogenesis. Xenotransplantation of tumor-derived mural-like cells (GSDCs) expressing YKL-40 in mice developed extensive and stable blood vessels covered with more GSDCs than those in YKL-40 gene knockdown tumors. YKL-40 expressed by GSDCs was associated with increased interaction of neural cadherin/β-catenin/smooth muscle alpha actin; thus, mediating cell-cell adhesion and permeability. YKL-40 also induced the interaction of vascular endothelial cadherin/β-catenin/actin in endothelial cells (HMVECs). In cell co-culture systems, YKL-40 enhanced both GSDC and HMVEC contacts, restricted vascular leakage, and stabilized vascular networks. Collectively, the data inform new mechanistic insights into the cooperation of mural cells with endothelial cells induced by YKL-40 during tumor angiogenesis, and also enhance our understanding of YKL-40 in both mural and endothelial cell biology.

Keywords

YKL-40; N-cadherin; VE-cadherin; VEGF; endothelial cells; mural cells; vessel permeability; vessel stability; tumor angiogenesis

*Corresponding author: Rong Shao, Ph.D. Pioneer Valley Life Sciences Institute University of Massachusetts Amherst Springfield, MA 01107 Fax: 413-794-0857 rong.shao@bhs.org.

Conflict of interest: The authors declare no conflict of interest.

Introduction

Neo-vascular networks function to deliver nutrients, oxygen, and other molecules to developmental tissue or pathologic lesion, the process known to mediate vasculogenesis and angiogenesis (1, 2). The key step of this event involves the formation of the neo-vasculature wall that is primarily composed of both endothelial cells and mesenchyme-derived mural cells including smooth muscle cells and/or pericytes (3). In physiological angiogenesis (*e.g.* wound healing), endothelial cells initially sprout to form neo-vessels followed by recruitment of mural cells in a paracrine manner dependent on PDGFB-PDGFRβ and angiopoietin-1-Tie-2 reciprocal activation (4, 5). It is acknowledged that vasculature in the central nervous system contains the highest amount of mural cell coverage (6).

Once mural cells are recruited onto the abluminal surface of endothelial cell-based vessels, intercellular junctions between endothelial cells, mural cells, and/or endothelial-mural cells act as a central factor to render the vascular network mature and stable. A number of intercellular adhesion molecules are appreciated to regulate vessel fenestration, permeability, and stability. For instance, vascular endothelial cadherin (VE-cadherin) plays an important role in controlling endothelial-to-endothelial cell contacts (7–9), while neural cadherin (N-cadherin) mediates endothelial-to-mural cell and mural-to-mural cell communication (10–12). A key intracellular mediator of the cadherin-associated cell-to-cell contacts is β-catenin that acts as a physical link to the cytoskeleton assembly including actin (13, 14). Disruption of the complex between cadherins and β-catenin results in decreased cell-cell interactions and increased cell permeability. Other gap junction proteins such as claudins, occludin, and connexins also participate in distinct intercellular interactions (3, 6). The spatial cooperation and regulation of these cell-cell tight contacts commit endothelial cells and mural cells to orchestrate the vessel wall, which offers adequate nutrients and oxygen for tissue proliferation.

Although it remains to be clarified if different identities and/or functions of mural cells exist between tumor and normal vessels, chaotic vasculature with either abundant or insufficient coverage of mural cells is frequently observed during tumor angiogenesis (15). Deletion of mural cells in tumor-bearing mice exhibited an impaired vascular phenotype with diminished mature vessel formation and increased vessel permeability, thus retarding tumor progression (16, 17). As the most potent angiogenic factor, vascular endothelial growth factor (VEGF), also known as a vascular permeability factor, promotes endothelial permeability and destabilizes vascular integrity via interrupting VE-cadherin function in endothelial cells (18, 19). In light of VEGF activity in mural cell coverage of tumor vessels, there is strong evidence indicating that ablation of myeloid cell-derived VEGF in mice led to increased mural cell coverage of the vessels and acceleration of tumorigenesis. These findings unveil a new pathologic signature of VEGF in functional inhibition of mural cell-associated vessels (20, 21).

YKL-40 (human cartilage glycoprotein-39 or chitinase-3-like-1) is a secreted glycoprotein that was originally identified from culture medium of a human osteosarcoma cell line MG-63 (22). Human YKL-40 protein contains an open reading frame of 383 amino acids with a molecular mass of 40 kDa and it is a member of glycoside hydrolase family 18 that

contains chitinases. But YKL-40 can only bind chitin-like oligosaccharides and does not have chitinase/hydrolase activity because of the substitution of an essential glutamic acid with leucine in the chitinase-3-like catalytic domain (23, 24). YKL-40 is normally expressed by different cell types such as vascular smooth muscle cells (25), macrophages (26), neutrophils (27), chondrocytes (28), and synoviocytes (29). To date, its biophysiological function in those cells including mesenchyme-derived mural cells/vascular smooth muscle cells is incompletely understood.

Multiple independent studies have shown that high serum levels of YKL-40 are correlated with metastasis and poor survival in a broad spectrum of human carcinomas including breast cancer (30), colorectal cancer (31), ovarian cancer (32), leukemia (33), lymphoma (34), and glioblastoma (35), suggesting that serum levels of YKL-40 serve as a diagnostic and prognostic cancer biomarker. We have recently demonstrated that YKL-40 acts as an angiogenic factor to stimulate vascular endothelial cell development in breast cancer and brain tumors (36, 37). YKL-40 is also known to be associated with tumor mesenchymal transition, displaying a poor prognosis (38). However, it is largely unknown how YKL-40-induced neo-vessels are stabilized to be functional and what the role of YKL-40 plays in tumor vasculogenesis characterized by communication between endothelial cells and mural cells. Here, we sought to explore the molecular mechanisms through which YKL-40 controls vascular permeability, stability, and angiogenesis mediated by mural cells in addition to vascular endothelial cells. To achieve this purpose, we took advantage of our recently established tumor cells named GSDC that are originally derived from human brain tumors and behave as vascular mural-like cells (39). This model demonstrates 1) tumors with vigorous vasculature when they are transplanted in animals; 2) a mesenchymal phenotype strongly expressing YKL-40, smooth muscle actin alpha (SMa), PDGFRβ, and vimentin; and 3) YKL-40 expressed by mural-like cells acts as a key factor regulating tumor vascularization. The current study has informed a key role of YKL-40 in both mural cell and endothelial cell biology during tumor angiogenesis.

Results

Tumor vascular coverage, stability, and angiogenesis are dependent on GSDCs expressing YKL-40

To interrogate if YKL-40, a mesenchymal marker expressed by mural-like cells, GSDCs, acts as a central factor to establish vessel stability and integrity during tumor angiogenesis, we began our study by employing a gene knockdown approach utilizing a retroviral infection of shRNA against the YKL-40 gene in GSDCs. Two shRNA constructs sufficiently suppressed YKL-40 expression by over 90% compared to a shRNA scrambled control, as examined by western blotting (Supplemental Fig. 1A). Accordingly, YKL-40 gene knockdown led to decreased expression of SMa, a mural cell marker, and cell motility (Supplemental Fig. 1A–1C).

To investigate a potential role of YKL-40 in tumor vascular stability, permeability, and angiogenesis *in vivo*, we engaged an orthotopic xenografted tumor model by injecting GSDCs expressing scramble RNA or one of YKL-40 shRNAs (shRNA 1) into the brains of SCID/Beige mice for a 5-month observation period. After the mice were sacrificed, we

examined tumor sections for angiogenesis by staining CD31, an endothelial cell marker. GSDC control tumors revealed a strong vascularized phenotype as an intense CD31-positive vessel density was found throughout the entire tumor region (Fig. 1A-a). In contrast, YKL-40 shRNA tumors displayed a significant reduction of the vessel density by approximately 60% (Fig. 1A-b & 1B). In addition, most of the vessels in the control tumors contained a visible lumen, whereas vessels in the YKL-40 shRNA tumors were collapsed and vessel diameters diminished to 30% relative to the control ones (Fig. 1A-a, b, & 1B). An analysis of mural cell coverage by co-staining CD31 and SMa indicated that over 90% of endothelial cell-based vessels in the control tumors were covered with mural cells, in comparison with less than 40% of vessels lined with mural cells in the YKL-40 shRNA tumors (Fig. 1A–c, d, & 1C). To distinguish vessels covered by the tumor-derived GSDCs from those by host-derived mural cells, we similarly injected GSDCs carrying green fluorescent protein (GFP) into different mice. The majority of endothelial cell vessels (CD31) were surrounded by GFP-positive GSDCs at the abluminal site where GFP and SMa were co-localized, while a few vessels were stained with CD31 only (Supplemental Fig. 2A–2F), suggesting that tumor-derived mural-like cells make a significant contribution to tumor vessel coverage. Consistent with this finding, YKL-40 was expressed by SMa-positive mural cells in addition to tumor cells (Supplemental Fig. 2H & 2I). Vessel permeability was measured by diffusion of fibrinogen from the blood circulation. A limited amount of fibrinogen was identified to be diffused out of capillaries in the control tumors, contrary to that in the YKL-40 shRNA tumors which contained more than 6-fold greater diffusion of fibrinogen, indicative of leakier vessels (Fig. 1A–e, f, & Fig. 1D). These *in vivo* data suggest that YKL-40 expressed by GSDCs mediates vascular mural cell coverage, stability, and angiogenesis.

To characterize effects of YKL-40 on tumor development, the tumors were tested for the proliferation marker Ki67. GSDC control tumors displayed positive staining of Ki67 by 3.3-fold greater than did YKL-40 shRNA tumors (Fig. 1E & 1F). Monitoring tumor cell growth in cultured condition revealed a decrease of cell proliferation by 10% in YKL-40 shRNA cells relative to counterparts (Fig. 1G), suggestive of partial contribution of YKL-40 to the cell growth. In concert with tumor growth and angiogenesis, mice receiving control cells showed a trend towards decreased overall survival as compared with YKL-40 shRNA mice over this 5-month trial (Fig. 1H). In sum, the *in vivo* animal models gave rise to evidence supporting our hypothesis that YKL-40 derived from mural-like cells plays a vital role in maintaining vascular permeability, stability, and angiogenesis in tumors through mural cell coverage; thus fueling tumor growth and development.

YKL-40 expression is associated with strong intercellular contacts and adhesion of GSDCs

To explore molecular mechanisms that possibly mediate intercellular contacts and vascular coverage found earlier *in vivo*, we examined expression and interaction of N-cadherin/β-catenin/SMa in control and YKL-40 shRNA GSDCs. While N-cadherin remained unchanged, expression of β-catenin and SMa was decreased when the YKL-40 gene was knocked down (Fig. 2A and Supplemental Fig. 1A). In control cells, VEGF production was barely detectable; but was dramatically up-regulated in YKL-40 shRNA cells. To determine

if the interaction of N-cadherin with β-catenin and its downstream effector SMa was diminished due to the decreased levels of β-catenin and SMa by YKL-40 shRNA, we performed a co-immunoprecipitation assay followed by immunoblotting. Both interactions of N-cadherin with β-catenin and β-catenin with SMa in control cells were stronger than those in YKL-40 shRNA cells (Fig. 2B). Accordingly, immunocytochemical analysis confirmed about two-fold higher association of N-cadherin with β-catenin in the control cells than that in the YKL-40 shRNA cells (Fig. 2C). Likewise, the similar association patterns of β-catenin with SMa were found in these cells by immunocytochemistry (data not shown). However, the reduced association of N-cadherin and β-catenin in the YKL-40 shRNA cells could not be rescued by VEGF neutralization. These results suggest that YKL-40 expression by GSDCs is associated with the interaction of N-cadherin, β-catenin, and SMa, independent of VEGF activity.

In order to determine if these altered cell-cell contacts lead to changes in intercellular adhesion activity, we measured cell aggregation. YKL-40 shRNA inhibited cell aggregation by 55% compared to a control level (Fig. 2D). Neutralizing N-cadherin via an anti-N-cadherin antibody in control GSDCs resembled the inhibition of YKL-40 shRNA, and combination of the N-cadherin blockade and YKL-40 shRNA slightly enhanced the inhibition on cell-cell adhesion, implying that N-cadherin may contribute a primary role to YKL-40-mediated cell to cell adhesion (Fig. 2D). Overall, these data underscore the importance of YKL-40 in the ability of GSDCs to maintain cell to cell junctions through the N-cadherin/β-catenin/SMa pathway.

GSDC-conditioned medium containing YKL-40 mediates intercellular contacts and adhesion of endothelial cells

To explore effects of YKL-40 expressed by GSDCs on intercellular junctions of vascular endothelial cells via a paracrine manner, we used conditioned media from control or YKL-40 shRNA GSDCs in the culture of human microvascular endothelial cells (HMVECs) and measured intercellular contacts of VE-cadherin and β-catenin. HMVECs expressed a stronger level of VE-cadherin than N-cadherin, suggestive of a main role of VE-cadherin in cell to cell contacts (Fig. 3A). The media from control and YKL-40 shRNA cells did not alter expression of VE-cadherin, N-cadherin, or β-catenin (Fig. 3A & Supplemental Fig. 3A). However, like GSDCs, co-immunoprecipitation studies showed that media from YKL-40 shRNA cells inhibited the interaction of VE-cadherin with β-catenin, and β-catenin with actin in HMVECs (Fig. 3B & Supplemental Fig. 3B). A minimal level of N-cadherin/β-catenin association was detected in HMVECs treated with conditioned media from either control or YKL-40 shRNA cells (data not shown). Because VEGF secretion was significantly elevated in the conditioned media from YKL-40 shRNA cells (Fig. 2A), the increased VEGF may contribute mainly to the reduced VE-cadherin/β-catenin interaction. To test this possibility, we used an anti-VEGF neutralizing antibody in the co-immunoprecipitation assay of HMVECs. VEGF blockade restored the association of VE-cadherin with β-catenin (Fig. 3B). Consistent with the co-immunoprecipitation data, HMVECs treated with conditioned medium of YKL-40 shRNA cells displayed reduced co-localization of VE-cadherin and β-catenin to 13% relative to control cell medium, and treatment with an anti-VEGF neutralizing antibody recovered the co-localization to

approximately 63% of the control levels (Fig. 3C & 3D). In addition, the cell aggregation analysis unveiled the similar inhibition of cell to cell adhesion (by 46–54%) by conditioned media from YKL-40 shRNA, control cells treated with a VE-cadherin neutralizing antibody, or YKL-40 shRNA cells treated a VE-cadherin antibody (Fig. 3E). To confirm the key role played by YKL-40 in endothelial cell to cell interaction, we also treated conditioned medium of the control GSDCs expressing YKL-40 with a neutralizing YKL-40 antibody (mAY) (40). The conditioned medium containing mAY abolished the interaction between VE-cadherin and β-catenin relative to the control mIgG medium (Fig. 3F). Accordingly, the control GSDC medium in the presence of mAY suppressed HMVEC aggregation by 60% compared to the aggregation in the presence of mIgG (Fig. 3G). While neither the neutralizing anti-VEGF antibody nor mAY altered expression of VE-cadherin, N-cadherin and β-catenin in HMVECs (data not shown), treatment of control GSDCs with mAY inhibited YKL-40 expression; in contrast, the anti-VEGF antibody in YKL-40 shRNA GSDCs induced VEGF (Supplemental Fig. 3C), suggestive of distinct responses of mural cells to individual inhibitors. Collectively, these data suggest that YKL-40 may induce the VEcadherin/β-catenin/actin pathway and cell to cell adhesion in endothelial cells, and that YKL-40 blockade inhibits these effects, which is largely dependent on VEGF.

YKL-40, in contrast to VEGF, stimulates interaction of VE-cadherin with β-catenin in HMVECs

In order to investigate the roles that YKL-40 and VEGF play individually in the association between VE-cadherin and β-catenin in HMVECs, we treated the cells with recombinant protein of VEGF or YKL-40. Treatment of HMVECs with YKL-40 or VEGF did not alter protein expression of VE-cadherin, N-cadherin, or β-catenin (data not shown). However, YKL-40 induced the interaction between VE-cadherin and β-catenin; in contrast, VEGF inhibited their association (Fig. 4A). The immunocytochemical analysis validated this result that YKL-40 significantly increased co-localization of VE-cadherin and β-catenin by 60% relative to the control, while VEGF treatment decreased their co-localization by 43% (Fig. 4B & 4C). In a trial using different concentrations of these proteins, VEGF (10 ng/ml) and YKL-40 (200 ng/ml) at the pathologic levels were found to have more effects on these adhesion molecule interactions than other concentrations (data not shown). The results indicate that YKL-40, in contrast to VEGF, induces the interaction of VE-cadherin and β-catenin in HMVECs, further supporting the earlier findings using GSDC-conditioned media expressing YKL-40.

YKL-40 expressed by GSDCs mediates the cadherin/catenin complexes in co-culture of GSDCs and HMVECs

To monitor the interaction of cadherin and catenin between endothelial cells and mural cells that may recapitulate their functional relationship in vessels *in vivo*, we undertook an immunocytochemical approach probing the co-localization of either VE-cadherin/β-catenin or N-cadherin/β-catenin in a cell co-culture system with GSDCs and HMVECs. Intense co-staining of VE-cadherin/β-catenin was found in HMVECs mixed with control GSDCs, but this co-localization was decreased by 58% in HMVECs when co-cultured with YKL-40 shRNA GSDCs (Fig. 5A), in which HMVECs were distinguished from GSDCs by positive

staining of VE-cadherin as indicated with white asterisks (Fig. 5A). This is indicative that YKL-40 expressing cells are crucial to VE-cadherin/β-catenin interaction in HMVECs.

Next, to determine the interaction between the N-cadherin and β-catenin in this co-culture system, we labeled GSDCs only with nuclear staining DAPI prior to mixing with HMVECs, because both cell types express N-cadherin and β-catenin. By this approach, we could discern GSDCs (DAPI-positive) from HMVECs (DAPI-negative), and analyzed individual GSDC-GSDC, HMVEC-HMVEC, and GSDC-HMVEC contacts (Fig. 5B, top & bottom left). Membrane co-localization of N-cadherin and β-catenin between control GSDCs was found around 38% of GSDC population, but this co-staining between YKL-40 shRNA GSDCs was reduced to 23% (around 40% reduction compared with the control) (Fig. 5B, bottom right). However, there was no appreciable difference of their co-localizations in other cell types. In line with the findings earlier using the single cell type system, the data suggest that YKL-40 mediates VE-cadherin/β-catenin association in HMVECs and N-cadherin/β-catenin complex in GSDCs.

YKL-40 expression by GSDCs is associated with restricted permeability of HMVECs and GSDCs

To further evaluate permeability of HMVECs and GSDCs, one of the key vascular functions, we utilized a permeability method that assays the ability of cells to be permeable to Dextran conjugated with FITC. First, we treated HMVECs with either conditioned media from control or YKL-40 shRNA GSDCs, and we found that control medium-treated HMVECs restricted the permeability that allowed FITC-Dextran to cross through the cells 30% less than did YKL-40 shRNA medium-treated cells (Fig. 6A, top graph). In order to verify the functional role of VE-cadherin in HMVEC permeability, we added a VE-cadherin neutralizing antibody to the media. While mIgG, as a control, did not have an impact in the permeability treated with control or YKL-40 shRNA media, a VE-cadherin antibody increased cell permeability in control medium-treated HMVECs (Fig. 6A, middle graph). However, this VE-cadherin neutralization in YKL-40 shRNA medium-treated cells failed to enhance the permeability induced by YKL-40 shRNA, consistent with HMVEC-HMVEC adhesion found earlier (Fig. 3E). This implies that VE-cadherin plays a key role in the elevated permeability of HMVECs treated with YKL-40 shRNA media. In order to determine the effect of VEGF on permeability, as VEGF mediated the disassociation of β-catenin from VE-cadherin (Fig. 3B–3D), we treated the HMVECs with an anti-VEGF neutralizing antibody. The anti-VEGF antibody fully reversed the GSDC YKL-40 shRNA medium-induced permeability to the level treated with GSDC control media (Fig. 6A, bottom graph). As expected, the anti-VEGF antibody did not have effects on the permeability of control medium-treated HMVECs because of the considerably lower level of VEGF in the control media. To validate this endothelial cell permeability restrained by YKL-40, we treated HMVECs with mAY in the presence of GSDC control medium and found that mAY induced HMVEC permeability by 51% (Supplemental Fig. 4A). These results suggest that YKL-40 maintains HMVEC permeability and that YKL-40 blockade destabilizes the permeability probably through VE-cadherin activation.

Next, we assessed impacts of YKL-40 on GSDC permeability. GSDCs expressing YKL-40 shRNA exhibited a much higher permeability than control GSDCs, as the permeability of YKL-40 shRNA GSDCs was increased by up to 58% at 4 hr (Fig. 6B, top graph). Inhibition of N-cadherin using an anti-N-cadherin neutralizing antibody resulted in a 25% and 20% elevation in the permeability of control and YKL-40 shRNA GSDCs, respectively, compared with mIgG treatment over the 4-hr observation (Fig. 6B, middle graph). Unlike an anti-VE-cadherin antibody in HMVECs (Fig. 6A, middle panel), blocking N-cadherin in YKL-40 shRNA GSDCs enhanced cell permeability (by 20% compared with YKL-40 shRNA), analogous with the adhesion result (Fig. 2D), suggesting that other cell adhesion factors, in addition to N-cadherin, may also participate in YKL-40-mediated cell adhesion and permeability. For example, inhibition of integrins αVβ3 or αVβ5 partially increased cell leakage relative to N-cadherin inhibition (Supplemental Fig. 4B). To further validate that VEGF contributes to HMVEC, but not GSDC, permeability, we treated GSDCs with an anti-VEGF antibody. As expected, this anti-VEGF antibody failed to have an effect on the permeability of control or YKL-40 shRNA GSDCs that express strong VEGF (Fig. 6B, bottom graph). These results suggest that YKL-40 stabilizes GSDC permeability in a manner mainly dependent on N-cadherin.

Finally, to evaluate the overall cell permeability mediated by both GSDCs and HMVECs that would be more representative of vessel function *in vivo*, we loaded either control or shRNA GSDCs first for 2 hours followed by plating HMVECs on the top of the GSDCs, which simulated the vascular orientation from an “endothelial cell to mural cell” layer and encountered penetration of FITC-Dextran. Co-cultured YKL-40 shRNA GSDCs with HMVECs induced the “vascular” permeability by 25% greater than that of the system containing HMVECs and control GSDCs (Supplemental Fig. 4C). To assess the role of VEGF in cell permeability, we treated both cells with an anti-VEGF antibody. Consistent with the results found in the single HMVEC system above, VEGF abrogation suppressed the permeability of HMVECs induced by YKL-40 shRNA GSDCs to the control level (Fig. 6C). Dual treatment with VE-cadherin and N-cadherin antibodies in HMVECs with either control GSDCs or YKL-40 shRNA GSDCs led to stronger increases in the permeability than that induced by YKL-40 shRNA GSDCs in the presence of mIgG (Fig. 6D), suggesting that combined activities of VE- and N-cadherin contribute predominantly to the vessel permeability. Collectively, all the data support the notion that YKL-40 controls vascular permeability by regulating VE-cadherin and N-cadherin function in endothelial cells and mural cells, respectively.

HMVEC-formed tubules are stabilized by GSDCs expressing YKL-40

In an attempt to assess if GSDCs indeed act as mural cells to stabilize endothelial cell vessels, we employed a tube formation assay on Matrigel by co-culturing both HMVECs and GSDCs. HMVECs pre-labeled with Calcein AM (green fluorescence) were mixed with either control or YKL-40 shRNA GSDCs pre-labeled with Calcein red (red fluorescence). Stability of tubules formed by HMVECs and GSDCs was monitored over a 64-hr time course. As shown in Fig. 7A, HMVECs co-cultured with control GSDCs maintained tubules longer than did HMVECs in the presence of YKL-40 shRNA GSDCs. The breakdowns and gaps in the tube network, indicated by arrows, were significantly less in HMVECs with

control GSDCs at 24 hours and 40 hours than corresponding HMVECs co-cultured with YKL-40 shRNA GSDCs (Fig. 7A & 7B). HMVECs alone maintained their own tubules only between 24–36 hr (data not shown). To further validate the individual role of VE-cadherin and N-cadherin in vascular stability, we treated this co-culture system with a VE-cadherin or N-cadherin neutralizing antibody. When HMVECs co-cultured with control GSDCs were treated with either cadherin antibody, tubule stability was decreased to the level seen in the co-culture of HMVECs and YKL-40 shRNA GSDCs (Fig. 7C & Supplemental Fig. 5). As expected in the system of HMVECs and YKL-40 shRNA GSDCs, anti-VE-cadherin and N-cadherin antibodies were unable to influence the stability because of impaired activity of VE-cadherin and N-cadherin by YKL-40 gene knockdown. To determine a role of VEGF in the co-culture system, we treated HMVECs and control GSDCs with recombinant VEGF, and we found that the addition of VEGF to the YKL-40-expressing system developed more stabilized tubules than did control counterparts (Fig. 7C & Supplemental Fig. 5). The phenotype of elevated tubes is probably due to the synergistic cooperation of these two strong angiogenic factors for the tube generation and stabilization, as the vessel-destabilized property of VEGF may be notably minimized in the presence of YKL-40. An anti-VEGF antibody partially rescued the tube stability formed by HMVECs and YKL-40 shRNA cells that express a high level of VEGF. Failure of full tubule recovery in the presence of the anti-VEGF antibody is attributed to impaired N-cad function, even when VEGF is inhibited. Thus, these data suggest that the ability of GSDCs to stabilize endothelial cell-based vasculature is reliant on YKL-40 expression that regulates VEGF, VE- and N-cadherin activity. Altogether, in coordination with tumor vasculature found *in vivo*, the *in vitro* system identifying cell-cell contacts/adhesion, permeability, and stability of vascular wall cells have provided the critical mechanisms strengthening our conclusion that YKL-40 plays a central role in mural cell-mediated tumor angiogenesis via autocrine and paracrine loops.

Discussion

We previously demonstrated that YKL-40 can induce endothelial cell angiogenesis in tumors (36). Here, we have provided substantial evidence using brain tumor-derived mural-like cells to uncover a new angiogenic role of YKL-40 in tumor vascular permeability, stability, and activity characterized by the intimate interaction between endothelial cells and mural cells. This finding was also supported by the identical mural-like characteristics of brain tumor cells from different patients (data not shown). The reason for selecting such mesenchyme-derived mural cells is because a considerable subset of brain tumors (*e.g.* glioblastomas) express strong YKL-40 and demonstrate poorer prognosis with a mesenchymal phenotype and vigorous vascularization (37, 38). In addition, the vasculature of the central nervous system is typically covered with abundant mural cells in angiogenesis (6). Thus, the current study has advanced our knowledge about YKL-40 in both mesenchymal mural cell and vascular endothelial cell biology during tumor vascularization. Furthermore, understanding the regulation of the intercellular junctions that mediate the interaction between endothelial cells and mural cells, rather than focusing on endothelial cells alone, has offered additional mechanistic insights into the entity of the angiogenic process induced by YKL-40 in tumor microenvironment.

In physiological angiogenesis, bone marrow-derived progenitor cells or myofibroblastic precursors are appreciated as the primary mesenchymal origin capable of differentiating into mural cells that involve vessel maturation (41–43). However, in tumor angiogenesis, transplanted tumor cells expressing mesenchymal markers YKL-40, SMa, and vimentin were found to serve as a major component of mesenchymal mural cells. This is the first time in our knowledge to provide evidence indicating that tumor-derived mural-like cells may functionally substitute host-derived mesenchymal mural cells that are presumably deregulated in the scenario of highly vascular proliferation. Therefore, the evidence enhances our understanding of potential functional and genetic differences in different mural cell identities such as mesenchymal tumor-derived mural cells *vs*. host mesenchyme-differentiated mural cells. YKL-40 supports vessel stability and maintains vascular integrity mainly through activation of the N-cadherin/β-catenin/SMa and VE-cadherin/β-catenin/Actin pathway in mural-to-mural cell and endothelial-to-endothelial cell contacts, respectively. YKL-40 gene knockdown impaired these junctions, leading to vessel collapse and leakage, as a schematic model is illustrated in Fig 8. To further support this model, an additional study *in vivo* assaying vessel perfusion and oxygenation by injection of a hypoxia probe will be essential. By this approach, dysfunction of tumor perfusion and oxygenation ascribed to YKL-40 gene knockdown can be visualized. Thus, the characterization of tumor vascular development *in vivo*, in context with the present findings from vascular permeability and stability models using the co-culture systems, demonstrates that elevated YKL-40 mediates vascular mural cell coverage, stability, and angiogenesis; ultimately fostering tumor cell proliferation. These findings underscore a key role of YKL-40 in the establishment of tumor angiogenesis mediated by the coordination of mural cells with endothelial cells. Indeed, focusing on mural cell-mediated vessel coverage and stabilization has recently received significant attention in tumor neo-vascularization, the event that renders tumor cells evasive during the conventional anti-angiogenic therapy. For example, melanoma deficient of mural cells exhibited a leakier vascular phenotype and were more sensitive to an anti-VEGF drug Bevacizumab than the tumors that harbored mural cell-covered vessels (44), highlighting a protective role of mural cells in exposure to an anti-angiogenic drug. Whether or not YKL-40-stabilized vessels play the identical role in the drug resistance remains to be clarified, as it may hold therapeutic promise in patients who do not respond to angiogenesis-blocking agents.

VEGF, a strong permeability factor, stimulates angiogenesis and tumor growth through enhancing endothelial cell migration, proliferation, survival as well as vessel permeability or destabilization of endothelial-to-endothelial cell contacts (45, 46). VEGF-induced vessel permeability is associated with VE-cadherin tyrosine phosphorylation and degradation. VEGF binds its membrane tyrosine kinase receptor 2 (Flk-1) and induces Flk-1 tyrosine phosphorylation and activity that can activate VE-cadherin by Src-dependent tyrosine phosphorylation (47–49). Subsequently, the activated VE-cadherin disassociates from Flk-1 and β-catenin, and is internalized to the cytoplasm where it is degraded. Thus, VE-cadherin phosphorylation leads to the loss of cell-cell junctions and the increase in cell permeability (50–52). Our current studies have provided multiple relevant results supporting this mechanism. For example, stimulation of endothelial cells with VEGF reduced the association between VE-cadherin and β-catenin, and treatment with an anti-VEGF antibody

in YKL-40 shRNA cells over-expressing VEGF facilitated the interaction of VE-cadherin with β-catenin. VE-cadherin blockade led to increased endothelial cell permeability, the effect identical to treatment of these cells with YKL-40 shRNA medium expressing high levels of VEGF. In addition, this VE-cadherin neutralization failed to enhance endothelial cell permeability induced by YKL-40 shRNA medium, suggesting that functional loss of VE-cadherin mediates VEGF-induced cell permeability. It is emerging that VEGF exhibits distinct impacts on endothelial cells and mural cells. Although we did not find effects of VEGF on GSDC permeability, there is evidence demonstrating inhibitory effects of VEGF on mural cell coverage of the vessels, thereby suppressing tumor development (20, 21). We also interestingly found that expression of β-catenin and SMa, in contrast to VEGF, was down-regulated in YKL-40 shRNA cells, suggesting that YKL-40 differentially regulates their expressions. Intracellular pathways mediating SMa and VEGF expression involve PI3K and/or MAPK signaling, as a PI3K inhibitor Wortmannin or MAPK inhibitor PD98059 blocked their expression in GSDCs (Supplemental Figure 6). This finding is consistent with our previous reports that PI3K-Akt and MAPK Erk-1 and Erk-2 mediate YKL-40 signaling in the regulation of angiogenesis and cell survival in U87 cells and GSDCs (37, 39–40). It is also interesting to interrogate if a membrane receptor specific for YKL-40 mediates the activation and expression of these molecules, as it is likely that the YKL-40 receptor interacts and coordinates with its adjacent cadherins to induce intracellular signaling pathways.

We utilized GSDCs derived from a glioblastoma patient and found this population participates in the vascular stability and permeability, functioning as mural cells. YKL-40 shRNA led to induction of VEGF, which seems to conflict with our previous findings in which YKL-40 up-regulates VEGF in glioblastoma cells U87, a commercially available tumor cell line (37). A number of possibilities might account for this discrepancy observed in the different studies. First, the heterogeneity of tumor could contribute to the difference of VEGF expression and its regulation by YKL-40, as glioblastomas contain several cell subpopulations such as astrocytes, neurons, and oligodendrocytes, in addition to other vascular cells and immune cells. Expression of VEGF is higher in U87 cells than that in GSDCs and another glioblastoma cell line SNB-75 (data not shown). Indeed, YKL-40 and VEGF expression vary in individual glioblastoma patients (37). Second, the elevation of VEGF in GSDCs expressing YKL-40 shRNA may represent a compensating effect in angiogenic responses during a chronic course of YKL-40 blockade, the event resembling the neutralization of VEGF in U87 cells that also increased YKL-40 expression (37). Neutralizing VEGF in YKL-40 shRNA GSDCs led to induction of VEGF expression, although the neutralized VEGF is not functional, supporting the compensating responses of the cells to their severely impaired angiogenic activities. Thus, those two vascular promoting factors coordinate and regulate each other to render tumors vascularized. Supporting this speculation, VEGF induced by YKL-40 in U87 cells stimulated endothelial cell tube formation, while in this study we primarily focused on VEGF in endothelial cell permeability, these different events cooperative for angiogenesis. In addition, adding VEGF to the co-culture system of YKL-40-expressing control GSDCs and HMVECs induced and stabilized vascular tubes (Fig. 7C). It is currently unknown which factor expressed differentially by U87 and GSDCs plays a key role in the regulation of VEGF that

divergently induces angiogenesis through the different cells. HIF-1α is not a core factor to contribute to the differential expression of VEGF in both cells (data not shown). Finally, even though it is currently unknown if U87 cells also mediate vascular stability via VEGF expression controlled by YKL-40, it is conceivable that multiple molecular mechanisms are involved in YKL-40-induced vascular stability and integrity, not limited to VEGF only. In the present study, we found that vascular stability contributed by GSDCs is dependent on N-cadherin, in contrast to endothelial cell-mediated permeability that depends on activation of VEGF-VE-cad. Therefore, the regulation between YKL-40 and VEGF in tumor vascularization relies on the function of individual cell populations that orchestrate tumor mass, vascular endothelium, and/or mural cell (vessel supporting) network.

Recent pre-clinical and clinical trials have established a therapeutic paradigm complementary to the conventional vessel-blocking regimen, in which normalization of tumor vascular abnormalities impedes tumor development (15). Depletion of mural cells in animal tumor models led to diminished blood vessels, increased tumor hypoxia, and restrained tumor growth (16). PDGF over-expression in patients was found to be associated with metastasis (53) and PDGF blockade that impairs mural cell recruitment was reported to improve drug delivery and chemotherapy (54, 55). It is also noteworthy that delivery of drugs targeting both endothelial cells (*e.g*. VEGFR inhibitor) and mural cells (*e.g*. PDGFRβ inhibitor) was more effective than individual anti-angiogenic drugs, because destabilizing vessels by inhibition of mural cell function rendered endothelial cells more susceptible to endothelial cell blockers (56, 57). Despite these promising data, conflicting evidence was also documented from several animal settings and clinical trials. For instance, deletion of mural cells promotes metastasis probably due to lack of a barrier preventing tumor cells from dissemination into the circulation system (58). Analogous with these findings, decreased mural cell coverage around vessels in patients is correlated with cancer metastasis (59). Although the molecular mechanisms underlying these distinct outcomes remain to be deciphered, the data suggest that multiple regulatory pathways be involved in the formation of tumor vascular network that demonstrates spatial-temporal deregulation of the interaction between endothelial cells and mural cells. Therefore, in the evaluation of drug delivery and therapy, several important factors mediating vascular maturation and normalization should be taken into account, such as vessel coverage, permeability and stability, interstitial fluid pressure, oxygen delivery, and local blood perfusion. Nevertheless, our current findings on YKL-40 in tumor angiogenesis characterized by coupling of mural cells to endothelial cells have demonstrated a potential therapeutic target in treatment of cancer patients that produce high levels of YKL-40.

Materials and Methods

Cell Culture

GSDCs established previously were grown in DMEM supplemented with 10% FBS and penicillin/streptomycin (39). HMVECs were grown in EBM-2 (Lonza, Allendale, NJ) supplemented with 5 μg/ml hydrocortisone, 10 ng/ml hEGF, 10% FBS, and penicillin/streptomycin.

YKL-40 Gene knockdown

DNA oligos (19 bp) specifically targeting N-terminal (siRNA 1) or C-terminal (siRNA 2) region of YKL-40, were selected and then templates (64 oligo nucleotides) containing these oligos were subcloned into a retroviral pSUPER-puro-vector (OligoEngine, Seattle, WA) (40). 293T retroviral packaging cells were transfected with pSUPER siRNA constructs in the presence of pCL 10A1 vector using Fugene 6 (Roche, Indianapolis, IN). Forty-eight hours after transfection, the supernatant was harvested and filtered through 0.45-μm pore size filter and then the viral medium was used to infect targeted cells. Selection with 1 μg/ml of puromycin was started 48 hr after infection and the puromycin-resistant cell populations were used for subsequent studies.

Immunoprecipitation and immunoblotting

Cell lysate samples were processed as described previously (60). Samples were subjected to running SDS-PAGE and PVDF membranes were incubated with one of a series of primary antibodies against N-cadherin, VE-cadherin (Invitrogen, Carlsbad, CA), β-catenin (Santa Cruz Biotechnology, Santa Cruz, CA), YKL-40 (our lab), VEGF (Sigma, St. Louis, MO), SMa (Abcam, Cambridge, MA), and actin (Sigma). Membranes were then incubated with goat anti-mouse or anti-rabbit secondary antibodies (Jackson Lab, Bar Harbor, Maine). Specific signals were detected by enhanced chemiluminescence (VWR, Rockford, IL). For immunoprecipitation, cell lysates were incubated with either an anti-VE-cadherin, N-cadherin, or β-catenin antibody at 4°C overnight followed by incubation with protein G Sepharose 4 Fast Flow beads at 4°C for 4 hr. The immunocomplex was extensively washed and the samples were run for immunoblotting as described earlier.

RT-PCR

Total RNA from cells was extracted with Tri-reagent (Molecular Research Inc, Cincinnati, OH). RNA concentration and purity were determined spectrophotometrically ($A_{260/280}$). cDNAs with poly A tails were subsequently synthesized through a reverse transcriptional reaction in the presence of 15-oligo (dT) (Promega, Madison, WI). A fragment of VEGF and GAPDH DNA was synthesized by a polymerase chain reaction with sense primer 5'-CTTTCTGCTGTCTTGGGTGC-3' and antisense primer 5'-GTGCTGTAGGAAGCTCATCTCTCC-3', and sense primer 5'-ATGGGGAAGGTGAAGGTCGGA-3' and antisense primer 5'-CTCCTTGGAGGCCATGT-3', respectively.

MTS Assay

Cellular proliferation was measured using Cell Titer 96 Aqueous Nonradioactive Cell Proliferation Assay Kit (Promega, Madison, WI) per the manufacturer's instructions. Briefly, GSDCs (2×10^3 cells) were plated onto a 96 well plate and allowed to grow overnight. The next day, the MTS reagent was added to the cells and incubated at 37° C for 1 hour. The plate was read at 490 nm absorbance to determine cell proliferation.

Cell permeability

HMVECs or GSDCs (2×10^5cells) were loaded onto 0.4-μm 24-transwells pre-coated with 100 μg/ml collagen IV overnight. For cell co-culture, GSDCs (1×10^5cells) were loaded for 2 hr prior to HMVECs (1×10^5cells). 24 hr later, Dextran conjugated with FITC (0.4 mg/ml, Invitrogen) was added on the top of the wells for 4 hr. At various time points, an aliquot from the bottom of the wells was measured for absorbance at 485 μm.

Immunocytochemistry

The method was described previously (61). Briefly, cells were grown to sub-confluence and fixed with 4% paraformaldehyde for 5 min. After permeabilization with Triton 100X, the cells were incubated with an anti-N-cadherin or VE-cadherin monoclonal antibody (1:100, Invitrogen) at 4°C overnight followed by incubation with a secondary anti-mouse or rabbit Alexa Fluor 488 or Alxa Fluor 555 antibody (1:1000, Invitrogen) for 2 hr. Cell nuclei were stained with DAPI. For dual staining, after incubation of the first antibody, the samples were then incubated with a polyclonal anti-β-catenin (1:100, Santa Cruz) or SMa antibody (1:100, Abcam) as described earlier. Positive staining in a single cell was defined based on each cell recognized by nuclear staining of DAPI. The positive signal from a viewed field was quantified with software ImageJ and then normalized with total cell numbers positive for DAPI. In some of dual-cell culture staining analyses, in addition to nuclear DAPI counted for cell number, a specific cell marker (*e.g.* VE-cad for endothelial cells) was also used to distinguish marker-positive cells from marker-negative cells. Images were analyzed using a Nikon TE2000U inverted fluorescent microscope.

Tube formation

HMVECs (2×10^4cells) were transferred onto 96-well Matrigel (BD Bioscience, San Jose, CA). After 16 hours of incubation, tube-forming structures were analyzed. Images were analyzed with an inverted microscope. Averages of tubules were calculated from three fields in each sample. For the vascular stability assay, HMVECs (2×10^4cells) and GSDCs (2×10^3cells) pre-labeled with Calcein AM and Calcein Red (5 μg/ml, Invitrogen), respectively, were mixed and loaded onto 96-well Matrigel over 64 hours. Tubules with fluorescence were imaged and quantified at various time points.

Cell aggregation

GSDCs or HMVECs (2×10^6) were re-suspended in 1 mL of serum-free media containing 1mM $CaCl_2$ and transferred to a 2-mL Eppendorf tube. The tube was placed in a shaker at 90 rpm at 37°C for 1 hour. Finally, cells were transferred to a cell culture dish for phase contrast imaging of cell aggregation. Aggregates were counted as colonies of 10 cells or more.

Scratch wound migration

GSDCs were plated at 95% confluency on a 24-well plate and allowed to grow overnight. A sterile 200 μL tip was then used to make a scratch through the middle of the well. The wells were washed gently twice with PBS to remove floating cells. Images were taken at time points 0 and 24 hr and the number of cells that migrated into the scratch was quantified.

Tumor xenografts in mice

All animal experiments were performed under the approval of Institutional Animal Care and Use Committee of the University of Massachusetts. GSDCs expressing control vector or YKL-40 shRNA (1.5×10^5) cells in 0.2 ml of PBS were injected into right striatum of SCID/Beige mice. Mice were sacrificed when mice displayed decreased locomotion.

Immunohistochemistry and immunofluorescence

Paraffin-embedded or frozen tumor tissue were cut to 6 μm thickness and processed for immunohistochemical analysis. In brief, samples were incubated with 3% H_2O_2 for 30 min to block endogenous peroxidase activity, followed by incubation with blocking buffer containing 10% goat serum for 1 hr. The samples then were incubated at room temperature for 2 hr with a rabbit polyclonal anti-Ki67 antibody (1:100, Invitrogen). A goat anti-rabbit secondary antibody (1: 100, Dako Inc, Carpinteria, CA) conjugated to HRP was added for one hr. Finally, DAB substrate (Dako Inc) was introduced for several minutes and after washing, methyl green was used for counterstaining. For a single and dual immunofluorescent staining, tumor specimens were incubated with a rat anti-CD31 (1: 50, BD Pharmingen, San Diego, CA) antibody for 2 hr followed by incubation with a goat anti-rat Alexa Fluor 555 secondary antibody (1: 250) for 1 hr. Then the samples were similarly incubated with a mouse anti-SMa (1:500, Dako Inc) or rabbit anti-fibrinogen antibody (1: 100, Dako Inc) followed by incubation with a goat anti-mouse or rabbit Alexa Fluor 488 antibody (1: 250) for 1 hr. Finally, DAPI was added to stain nucleus. NIH ImageJ software was used to quantify vessel density in the single staining of CD31, individual density of SMa, CD31, and fibrinogen in dual staining.

Statistics

Data are expressed as mean ± SE and n refers to the numbers of individual experiments performed. Differences among groups were determined using one-way ANOVA analysis followed by the Newman-Keuls test. The 0.05 level of probability was used as the criterion of significance.

Supplementary Material

Refer to Web version on PubMed Central for supplementary material.

Acknowledgments

This work was supported by NCI R01 CA120659 and CEAR grant, John Adams Innovation Institute, Massachusetts (RS).

Abbreviation

YKL-40	human cartilage glycoprotein-39 or Chitinase-3-like-1
N-cadherin	neural cadherin
VE-cadherin	vascular endothelial cadherin

VEGF	vascular endothelial growth factor
shRNA	short-hairpin RNA gene knockdown

References

1. Hanahan D. Signaling vascular morphogenesis and maintenance. Science. 1997; 277:48–50. [PubMed: 9229772]
2. Hanahan D, Folkman J. Patterns and emerging mechanisms of the angiogenic switch during tumorigenesis. Cell. 1996; 86:353–364. [PubMed: 8756718]
3. Jain RK. Molecular regulation of vessel maturation. Nat Med. 2003; 9:685–693. [PubMed: 12778167]
4. Hellstrom M, Gerhardt H, Kalen M, Li X, Eriksson U, Wolburg H, Betsholtz C. Lack of pericytes leads to endothelial hyperplasia and abnormal vascular morphogenesis. Journal of Cell Biology. 2001; 153:543–553. [PubMed: 11331305]
5. Bloch W, Huggel K, Sasaki T, Grose R, Bugnon P, Addicks K, Timpl R, Werner S. The angiogenesis inhibitor endostatin impairs blood vessel maturation during wound healing. FASEB Journal. 2000; 14:2373–2376. [PubMed: 11024009]
6. Armulik A, Genove G, Betsholtz C. Pericytes: developmental, physiological, and pathological perspectives, problems, and promises. Dev Cell. 2011; 21:193–215. [PubMed: 21839917]
7. Carmeliet P, Lampugnani MG, Moons L, Breviario F, Compernolle V, Bono F, Balconi G, Spagnuolo R, Oostuyse B, Dewerchin M, Zanetti A, Angellilo A, Mattot V, Nuyens D, Lutgens E, Clotman F, de Ruiter MC, Gittenberger-de Groot A, Poelmann R, Lupu F, Herbert JM, Collen D, Dejana E. Targeted deficiency or cytosolic truncation of the VE-cadherin gene in mice impairs VEGF-mediated endothelial survival and angiogenesis. Cell. 1999; 98:147–157. [PubMed: 10428027]
8. Dejana E, Orsenigo F, Lampugnani MG. The role of adherens junctions and VE-cadherin in the control of vascular permeability. Journal of Cell Science. 2008; 121:2115–2122. [PubMed: 18565824]
9. Orlova VV, Economopoulou M, Lupu F, Santoso S, Chavakis T. Junctional adhesion molecule-C regulates vascular endothelial permeability by modulating VE-cadherin-mediated cell-cell contacts. Journal of Experimental Medicine. 2006; 203:2703–2714. [PubMed: 17116731]
10. Paik JH, Skoura A, Chae SS, Cowan AE, Han DK, Proia RL, Hla T. Sphingosine 1-phosphate receptor regulation of N-cadherin mediates vascular stabilization. Genes & Development. 2004; 18:2392–2403. [PubMed: 15371328]
11. Gerhardt H, Wolburg H, Redies C. N-cadherin mediates pericyticendothelial interaction during brain angiogenesis in the chicken. Developmental Dynamics. 2000; 218:472–479. [PubMed: 10878612]
12. Luo Y, High FA, Epstein JA, Radice GL. N-cadherin is required for neural crest remodeling of the cardiac outflow tract. Developmental Biology. 2006; 299:517–528. [PubMed: 17014840]
13. Dejana E, Tournier-Lasserve E, Weinstein BM. The control of vascular integrity by endothelial cell junctions: molecular basis and pathological implications. Dev Cell. 2009; 16:209–221. [PubMed: 19217423]
14. Vestweber D. VE-cadherin: the major endothelial adhesion molecule controlling cellular junctions and blood vessel formation. Arteriosclerosis, thrombosis, and vascular biology. 2008; 28:223–232.
15. Carmeliet P, Jain RK. Principles and mechanisms of vessel normalization for cancer and other angiogenic diseases. Nat Rev Drug Discov. 2011; 10:417–427. [PubMed: 21629292]
16. Huang FJ, You WK, Bonaldo P, Seyfried TN, Pasquale EB, Stallcup WB. Pericyte deficiencies lead to aberrant tumor vascularizaton in the brain of the NG2 null mouse. Developmental Biology. 2010; 344:1035–1046. [PubMed: 20599895]
17. Abramsson A, Lindblom P, Betsholtz C. Endothelial and nonendothelial sources of PDGF-B regulate pericyte recruitment and influence vascular pattern formation in tumors. Journal of Clinical Investigation. 2003; 112:1142–1151. [PubMed: 14561699]

18. Weis S, Cui J, Barnes L, Cheresh D. Endothelial barrier disruption by VEGF-mediated Src activity potentiates tumor cell extravasation and metastasis. Journal of Cell Biology. 2004; 167:223–229. [PubMed: 15504909]

19. Gavard J, Gutkind JS. VEGF controls endothelial-cell permeability by promoting the beta-arrestin-dependent endocytosis of VE-cadherin. Nature Cell Biology. 2006; 8:1223–1234. [PubMed: 17060906]

20. Greenberg JI, Shields DJ, Barillas SG, Acevedo LM, Murphy E, Huang J, Scheppke L, Stockmann C, Johnson RS, Angle N, Cheresh DA. A role for VEGF as a negative regulator of pericyte function and vessel maturation. Nature. 2008; 456:809–813. [PubMed: 18997771]

21. Stockmann C, Doedens A, Weidemann A, Zhang N, Takeda N, Greenberg JI, Cheresh DA, Johnson RS. Deletion of vascular endothelial growth factor in myeloid cells accelerates tumorigenesis. Nature. 2008; 456:814–818. [PubMed: 18997773]

22. Johansen JS, Williamson MK, Rice JS, Price PA. Identification of proteins secreted by human osteoblastic cells in culture. Journal of Bone & Mineral Research. 1992; 7:501–512. [PubMed: 1615759]

23. Renkema GH, Boot RG, Au FL, Donker-Koopman WE, Strijland A, Muijsers AO, Hrebicek M, Aerts JM. Chitotriosidase, a chitinase, and the 39-kDa human cartilage glycoprotein, a chitin-binding lectin, are homologues of family 18 glycosyl hydrolases secreted by human macrophages. European Journal of Biochemistry. 1998; 251:504–509. [PubMed: 9492324]

24. Fusetti F, Pijning T, Kalk KH, Bos E, Dijkstra BW. Crystal structure and carbohydrate-binding properties of the human cartilage glycoprotein-39. Journal of Biological Chemistry. 2003; 278:37753–37760. [PubMed: 12851408]

25. Shackelton LM, Mann DM, Millis AJ. Identification of a 38-kDa heparin-binding glycoprotein (gp38k) in differentiating vascular smooth muscle cells as a member of a group of proteins associated with tissue remodeling. Journal of Biological Chemistry. 1995; 270:13076–13083. [PubMed: 7768902]

26. Rehli M, Krause SW, Andreesen R. Molecular characterization of the gene for human cartilage gp-39 (CHI3L1), a member of the chitinase protein family and marker for late stages of macrophage differentiation. Genomics. 1997; 43:221–225. [PubMed: 9244440]

27. Kzhyshkowska J, Gratchev A, Goerdt S. Human chitinases and chitinase-like proteins as indicators for inflammation and cancer. Biomarker insights. 2007; 2:128–146. [PubMed: 19662198]

28. Hu B, Trinh K, Figueira WF, Price PA. Isolation and sequence of a novel human chondrocyte protein related to mammalian members of the chitinase protein family. Journal of Biological Chemistry. 1996; 271:19415–19420. [PubMed: 8702629]

29. Nyirkos P, Golds EE. Human synovial cells secrete a 39 kDa protein similar to a bovine mammary protein expressed during the non-lactating period. Biochemical Journal. 1990; 269:265–268. [PubMed: 2375755]

30. Jensen BV, Johansen JS, Price PA. High levels of serum HER-2/neu and YKL-40 independently reflect aggressiveness of metastatic breast cancer. Clinical Cancer Research. 2003; 9:4423–4434. [PubMed: 14555515]

31. Cintin C, Johansen JS, Christensen IJ, Price PA, Sorensen S, Nielsen HJ. Serum YKL-40 and colorectal cancer. British Journal of Cancer. 1999; 79:1494–1499. [PubMed: 10188896]

32. Hogdall EV, Johansen JS, Kjaer SK, Price PA, Christensen L, Blaakaer J, Bock JE, Glud E, Hogdall CK. High plasma YKL-40 level in patients with ovarian cancer stage III is related to shorter survival. Oncology Reports. 2003; 10:1535–1538. [PubMed: 12883737]

33. Bergmann OJ, Johansen JS, Klausen TW, Mylin AK, Kristensen JS, Kjeldsen E, Johnsen HE. High serum concentration of YKL-40 is associated with short survival in patients with acute myeloid leukemia. Clinical Cancer Research. 2005; 11:8644–8652. [PubMed: 16361549]

34. Hottinger AF, Iwamoto FM, Karimi S, Riedel E, Dantis J, Park J, Panageas KS, Lassman AB, Abrey LE, Fleisher M, Holland EC, DeAngelis LM, Hormigo A. YKL-40 and MMP-9 as serum markers for patients with primary central nervous system lymphoma. Annals of neurology. 2011; 70:163–169. [PubMed: 21391238]

35. Pelloski CE, Mahajan A, Maor M, Chang EL, Woo S, Gilbert M, Colman H, Yang H, Ledoux A, Blair H, Passe S, Jenkins RB, Aldape KD. YKL-40 expression is associated with poorer response

to radiation and shorter overall survival in glioblastoma. Clinical Cancer Research. 2005; 11:3326–3334. [PubMed: 15867231]

36. Shao R, Hamel K, Petersen L, Cao QJ, Arenas RB, Bigelow C, Bentley B, Yan W. YKL-40, a secreted glycoprotein, promotes tumor angiogenesis. Oncogene. 2009; 28:4456–4468. [PubMed: 19767768]
37. Francescone RA, Scully S, Faibish M, Taylor SL, Oh D, Moral L, Yan W, Bentley B, Shao R. Role of YKL-40 in the angiogenesis, radioresistance, and progression of glioblastoma. The Journal of biological chemistry. 2011; 286:15332–15343. [PubMed: 21385870]
38. Phillips HS, Kharbanda S, Chen R, Forrest WF, Soriano RH, Wu TD, Misra A, Nigro JM, Colman H, Soroceanu L, Williams PM, Modrusan Z, Feuerstein BG, Aldape K. Molecular subclasses of high-grade glioma predict prognosis, delineate a pattern of disease progression, and resemble stages in neurogenesis. Cancer Cell. 2006; 9:157–173. [PubMed: 16530701]
39. Francescone R, Scully S, Bentley B, Yan W, Taylor SL, Oh D, Moral L, Shao R. Glioblastoma-derived Tumor Cells Induce Vasculogenic Mimicry through Flk-1 Protein Activation. The Journal of biological chemistry. 2012; 287:24821–24831. [PubMed: 22654102]
40. Faibish M, Francescone R, Bentley B, Yan W, Shao R. A YKL-40-neutralizing antibody blocks tumor angiogenesis and progression: a potential therapeutic agent in cancers. Molecular cancer therapeutics. 2011; 10:742–751. [PubMed: 21357475]
41. Chambers RC, Leoni P, Kaminski N, Laurent GJ, Heller RA. Global expression profiling of fibroblast responses to transforming growth factor-beta1 reveals the induction of inhibitor of differentiation-1 and provides evidence of smooth muscle cell phenotypic switching. American Journal of Pathology. 2003; 162:533–546. [PubMed: 12547711]
42. Tomasek JJ, Gabbiani G, Hinz B, Chaponnier C, Brown RA. Myofibroblasts and mechano-regulation of connective tissue remodelling. Nature Reviews Molecular Cell Biology. 2002; 3:349–363. [PubMed: 11988769]
43. Elenbaas B, Weinberg RA. Heterotypic signaling between epithelial tumor cells and fibroblasts in carcinoma formation. Experimental Cell Research. 2001; 264:169–184. [PubMed: 11237532]
44. Helfrich I, Scheffrahn I, Bartling S, Weis J, von Felbert V, Middleton M, Kato M, Ergun S, Schadendorf D. Resistance to antiangiogenic therapy is directed by vascular phenotype, vessel stabilization, and maturation in malignant melanoma. The Journal of experimental medicine. 2010; 207:491–503. [PubMed: 20194633]
45. Chen XL, Nam JO, Jean C, Lawson C, Walsh CT, Goka E, Lim ST, Tomar A, Tancioni I, Uryu S, Guan JL, Acevedo LM, Weis SM, Cheresh DA, Schlaepfer DD. VEGF-induced vascular permeability is mediated by FAK. Dev Cell. 2012; 22:146–157. [PubMed: 22264731]
46. Ferrara N, Kerbel RS. Angiogenesis as a therapeutic target. Nature. 2005; 438:967–974. [PubMed: 16355214]
47. Lambeng N, Wallez Y, Rampon C, Cand F, Christe G, Gulino-Debrac D, Vilgrain I, Huber P. Vascular endothelial-cadherin tyrosine phosphorylation in angiogenic and quiescent adult tissues. Circ Res. 2005; 96:384–391. [PubMed: 15662029]
48. Nakamura Y, Patrushev N, Inomata H, Mehta D, Urao N, Kim HW, Razvi M, Kini V, Mahadev K, Goldstein BJ, McKinney R, Fukai T, Ushio-Fukai M. Role of protein tyrosine phosphatase 1B in vascular endothelial growth factor signaling and cell-cell adhesions in endothelial cells. Circ Res. 2008; 102:1182–1191. [PubMed: 18451337]
49. Lin MI, Yu J, Murata T, Sessa WC. Caveolin-1-deficient mice have increased tumor microvascular permeability, angiogenesis, and growth. Cancer Res. 2007; 67:2849–2856. [PubMed: 17363608]
50. Shrivastava-Ranjan P, Rollin PE, Spiropoulou CF. Andes virus disrupts the endothelial cell barrier by induction of vascular endothelial growth factor and downregulation of VE-cadherin. Journal of virology. 2010; 84:11227–11234. [PubMed: 20810734]
51. Gorbunova E, Gavrilovskaya IN, Mackow ER. Pathogenic hantaviruses Andes virus and Hantaan virus induce adherens junction disassembly by directing vascular endothelial cadherin internalization in human endothelial cells. Journal of virology. 2010; 84:7405–7411. [PubMed: 20463083]
52. Shay-Salit A, Shushy M, Wolfovitz E, Yahav H, Breviario F, Dejana E, Resnick N. VEGF receptor 2 and the adherens junction as a mechanical transducer in vascular endothelial cells. Proceedings

of the National Academy of Sciences of the United States of America. 2002; 99:9462–9467. [PubMed: 12080144]

53. Liu J, Liao S, Huang Y, Samuel R, Shi T, Naxerova K, Huang P, Kamoun W, Jain RK, Fukumura D, Xu L. PDGF-D improves drug delivery and efficacy via vascular normalization, but promotes lymphatic metastasis by activating CXCR4 in breast cancer. Clin Cancer Res. 2011; 17:3638–3648. [PubMed: 21459800]
54. Jayson GC, Parker GJ, Mullamitha S, Valle JW, Saunders M, Broughton L, Lawrance J, Carrington B, Roberts C, Issa B, Buckley DL, Cheung S, Davies K, Watson Y, Zinkewich-Peotti K, Rolfe L, Jackson A. Blockade of platelet-derived growth factor receptor-beta by CDP860, a humanized, PEGylated di-Fab', leads to fluid accumulation and is associated with increased tumor vascularized volume. J Clin Oncol. 2005; 23:973–981. [PubMed: 15466784]
55. Hellberg C, Ostman A, Heldin CH. PDGF and vessel maturation. Recent results in cancer research. Fortschritte der Krebsforschung. 2010; 180:103–114. [PubMed: 20033380]
56. Erber R, Thurnher A, Katsen AD, Groth G, Kerger H, Hammes HP, Menger MD, Ullrich A, Vajkoczy P. Combined inhibition of VEGF and PDGF signaling enforces tumor vessel regression by interfering with pericyte-mediated endothelial cell survival mechanisms. FASEB Journal. 2004; 18:338–340. [PubMed: 14657001]
57. Bergers G, Song S, Meyer-Morse N, Bergsland E, Hanahan D. Benefits of targeting both pericytes and endothelial cells in the tumor vasculature with kinase inhibitors. Journal of Clinical Investigation. 2003; 111:1287–1295. [PubMed: 12727920]
58. Gerhardt H, Semb H. Pericytes: gatekeepers in tumour cell metastasis? Journal of molecular medicine (Berlin, Germany). 2008; 86:135–144.
59. Yonenaga Y, Mori A, Onodera H, Yasuda S, Oe H, Fujimoto A, Tachibana T, Imamura M. Absence of smooth muscle actin-positive pericyte coverage of tumor vessels correlates with hematogenous metastasis and prognosis of colorectal cancer patients. Oncology. 2005; 69:159–166. [PubMed: 16127287]
60. Yan W, Bentley B, Shao R. Distinct Angiogenic Mediators Are Required for Basic Fibroblast Growth Factor- and Vascular Endothelial Growth Factor-induced Angiogenesis: The Role of Cytoplasmic Tyrosine Kinase c-Abl in Tumor Angiogenesis. Molecular biology of the cell. 2008; 19:2278–2288. [PubMed: 18353972]
61. Yan W, Cao QJ, Arenas RB, Bentley B, Shao R. GATA3 inhibits breast cancer metastasis through the reversal of epithelial-mesenchymal transition. Journal of Biological Chemistry. 2010; 285:14042–14051. [PubMed: 20189993]

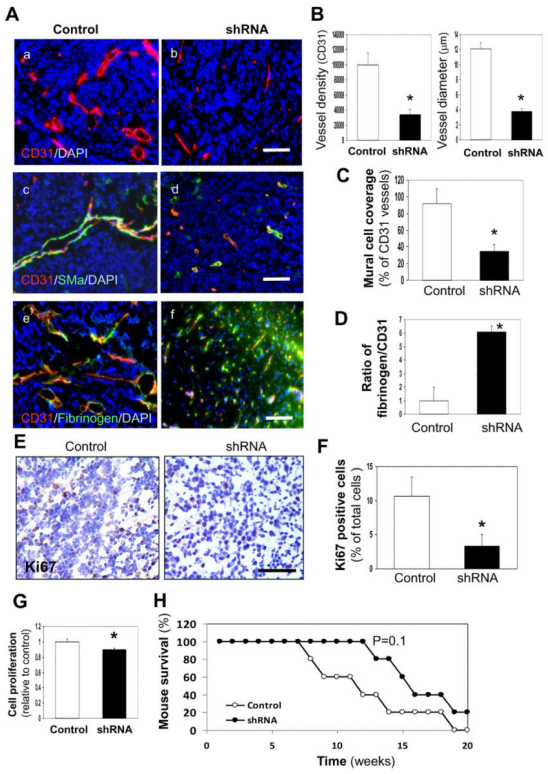

Figure 1. YKL-40 expression in GSDC-transplanted tumors is associated with vascular stability, mural cell coverage, angiogenesis, and tumor growth

A. Representative immunofluorescent images of control and YKL-40 shRNA GSDC brain tumor sections from SCID/Beige mice depicted single staining of CD31 (red) **(a, b)** and double staining of CD31 (red) with either SMa (green) **(c, d)** or fibrinogen (green) **(e, f)**. DAPI (blue) was used to stain the nuclei. **B.** Quantification of CD31 vessel density and vessel diameter from A (a, b) as described in the Methods. The latter was an average of individual luminal diameters. **C.** Quantification of percent mural cell coverage of CD31 vessels from A (c, d). The data were derived from the ratio of SMa density to CD31 density. **D.** Quantification of the ratio of fibrinogen *vs.* CD31 for vessel leakiness from A (e, f), in which the ratio of fibrinogen density to CD31 density in the control tumors was set as 1 unit. **E.** Representative control and YKL-40 shRNA GSDC tumor staining images of the proliferation marker Ki67. **F.** Percentage of Ki67 positive cells with brown nuclear staining was quantified. **G.** Cell proliferation in culture using MTS assay. N=12. **H.** Kaplan-Myer Survival curve of SCID/Beige mice bearing control or YKL-40 shRNA tumors. N=5. *P≤0.05 compared to corresponding controls. Bars: 100 μm.

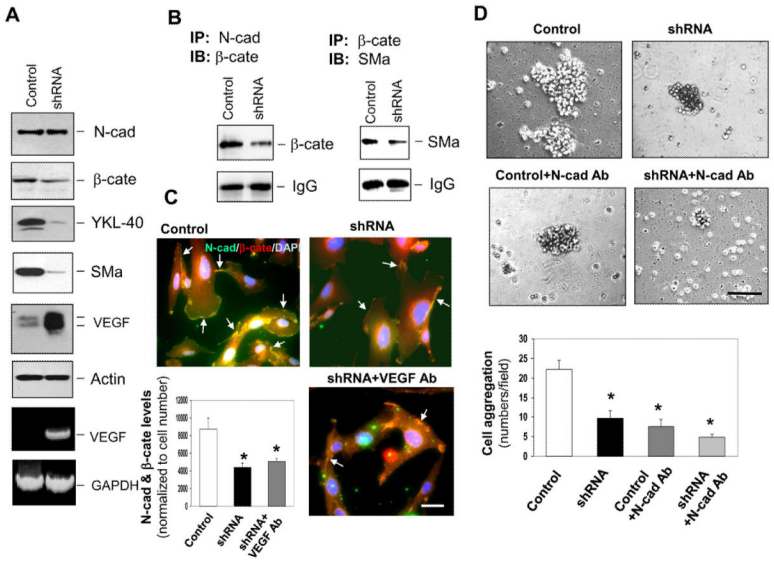

Figure 2. YKL-40 expression is associated with interaction of N-cadherin/β-catenin/SMa and cell-cell adhesion in GSDCs

A. GSDC control and YKL-40 shRNA cell lysates were probed for N-cadherin (N-cad), β-catenin (β-cate), YKL-40, SMa, VEGF, and actin expression through western blotting. VEGF mRNA levels were also tested by RT-PCR with GAPDH as a loading control. **B. (Left)** Immunoprecipitation of N-cad from control and YKL-40 shRNA cell lysates was tested for its association with β-cate by western blotting against β-cate. **(Right)** Immunoprecipitation of β-cate from control and YKL-40 shRNA cell lysates was tested for its association with SMa by western blotting against SMa. IgG protein levels were used to ensure equal levels of antibody pull down. **C.** GSDC control and YKL-40 shRNA cells were treated with or without a neutralizing anti-VEGF antibody (100 ng/ml) overnight. Immunocytochemistry of N-cad (green) and β-cate (red) to determine overlapping staining (yellow) indicated by arrows. Cell nuclei were stained by DAPI (blue). A bar: 10 μm. Quantification of co-staining between N-cad and β-cate by normalization of overlapping images to cell number. N=3, *P≤0.05 compared with control. **D.** Representative pictures of the cell aggregation assay. Cells were subjected to serum-free media with either IgG or an N-cad neutralizing antibody (Ab, 50 μg/ml) for one hour. Cell aggregates of 10 or more cells were counted for each condition and quantified below. A bar: 100 μm. N=3, * P≤0.05 compared with control.

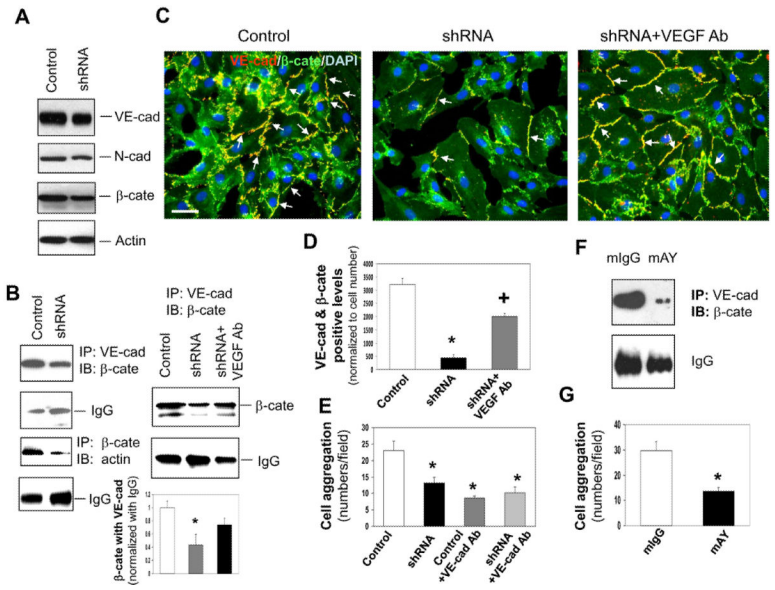

Figure 3. YKL-40 mediates the interaction of VE-cadherin/β-catenin/actin and cell-cell adhesion in HMVECs

A. Western blot analysis of VE-cad (VE-cad), N-cad, β-cate, and actin protein expression from the lysates of HMVECs treated with either control or YKL-40 shRNA GSDC-conditioned media for 24 hours. **B.** Immunoprecipitation of VE-cad from the HMVEC lysates treated for 24 hours with conditioned media from control, YKL-40 shRNA, or YKL-40 shRNA cells plus an anti-VEGF Ab (100 ng/ml) followed by immunoblotting of β-cate. IgG levels were used as a control. Immunoprecipitation of β-cate followed by immunoblotting against actin was similarly performed in HMVEC lysates. *P<0.05 compared with control. n=3. **C.** Double staining of VE-cad (red) with β-cate (green) in HMVECs treated with conditioned media from control, YKL-40 shRNA, or YKL-40 shRNA cells plus an anti-VEGF Ab to determine the extent of co-localization (yellow) indicated by arrows. Nuclei (blue) were stained by DAPI. A bar: 20 μm. **D.** Quantification of the immunocytochemistry images in part C, normalized to cell number. N=3, *P≤0.05 compared to control. $^{+}$P≤0.05 compared to control and YKL-40 shRNA. **E.** HMVEC aggregation was measured and quantified in the presence of GSDC control or YKL-40 shRNA media with an anti-VE-cad Ab (50 μg/ml). N=3, *P≤0.05 compared to control. **F.** HMVECs were treated with GSDC control medium in the presence of mAY or mIgG (10 μg/ml) overnight. Cell lystates were subjected to immunoprecipitation with an anti-VE-cadherin antibody followed by immunoblotting against β-cate. **G.** HMVECs treated with GSDC control medium in the presence of mAY or mIgG (10 μg/ml) were measured for cell aggregation. N=3, *P≤0.05 compared to control.

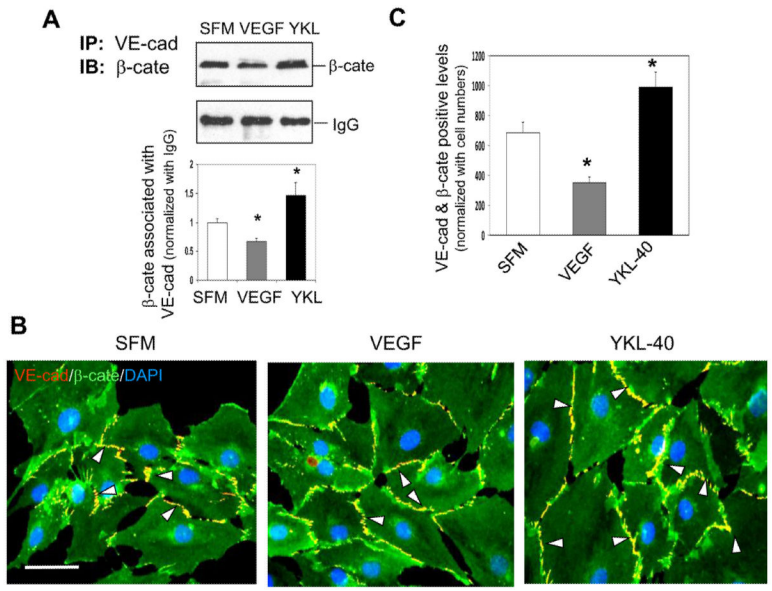

Figure 4. YKL-40 enhances interaction of VE-cadherin and β-catenin, but VEGF attenuates the interaction in HMVECs

A. (Top) HMEVC lysates treated 24 hr with serum-free medium (SFM) with or without 10 ng/mL VEGF, or 200 ng/mL recombinant YKL-40 were immunoprecipated with an anti-VE-cad Ab and probed for β-cate by western blotting. IgG was used as IP control. **(Bottom)** Quantification of the western blots above, normalized to IgG levels. *P<0.05 compared with SFM. n=3. **B.** Representative images of VE-cad (red) and β-cate (green) double stained HMVECs in the presence of either SFM, 10 ng/mL VEGF, or 200 ng/mL for 24 hr. White arrowheads highlight the areas positively co-stained for VE-cad and β-cate (yellow). **C.** Quantification of the VE-cad/β-cate overlap in the images in part C. A bar: 20 μm. N=3, *P≤0.05 compared to control.

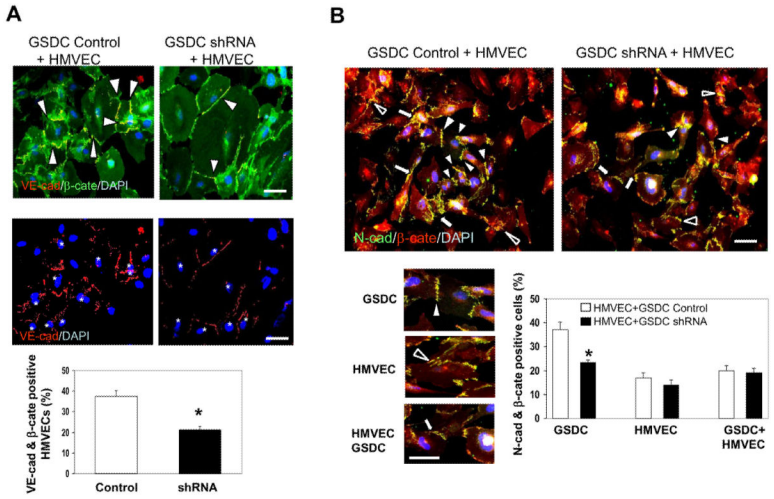

Figure 5. Co-culture of HMVECs and YKL-40-expressing GSDCs displays interaction between cadherin and catenin

A. (Top) HMVECs cultured with control or YKL-40 shRNA GSDCs were stained for VE-cad (red) and β-cate (green). White arrowheads mark regions of co-localization of VE-cad and β-cate. **(Middle)** VE-cad (red) staining was to show HMVECs distinct from VE-cad-negative GSDCs. White asterisks indicate HMVECs. DAPI (blue) was used as a nuclear stain for all images. **(Bottom)** Quantification of the percentage of HMVECs that have co-expression (yellow) of both VE-cad and β-cate in a total of HMVECs. Bars: 10 μm. N=3, *P≤0.05 compared to control. **B. (Top)** HMVECs and either control or YKL-40 shRNA GSDCs were cultured together and tested for overlapping of N-cad (green) and β-cate (red). DAPI was pre-stained for the nuclei of GSDCs only, but not for HMVECs to discriminate different cell types. **(Bottom, Left)** Representative images of the different types of cell to cell contacts: GSDC-GSDC (white arrowhead), HMVEC-HMVEC (black arrowhead), and HMVEC-GSDC (white arrow). **(Bottom, right)** Quantification of the percentage of cells containing N-cad/β-cate overlapping contacts in a total of individual cell types, displayed by cell contact types. Bars: 10 μm. N=3, *P≤0.05 compared to control.

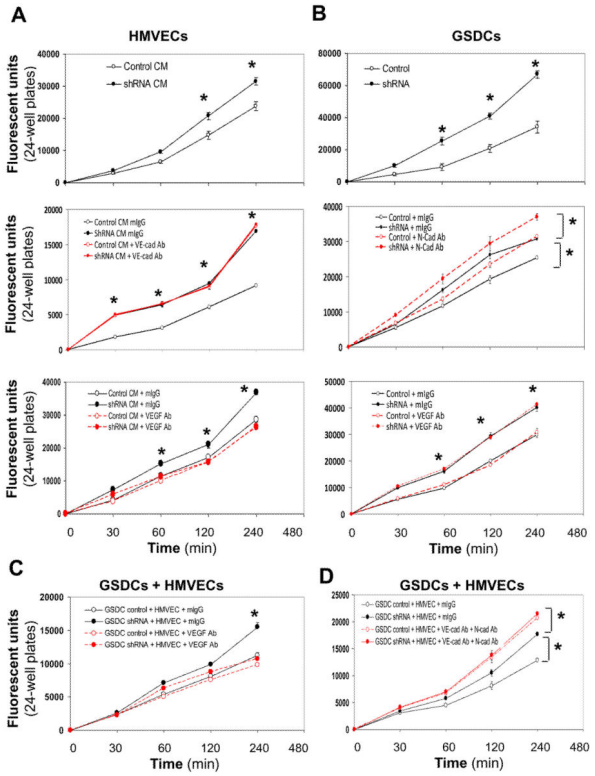

Figure 6. YKL-40 decreases permeability of HMVECs, GSDCs, and their combination in a manner dependent on VE-cad or N-cad activity

A. HMVECs were plated on inserts and allowed to attach and spread. Cells were treated overnight with either GSDC control conditioned media (CM, 24 hr serum-free media) or YKL-40 shRNA CM **(Top)**, control or YKL-40 shRNA CM with mouse IgG or an anti-VE-cad Ab (20 μg/ml) **(Middle)**, or anti-VEGF Ab (100 ng/ml) **(Bottom)**. Cell permeability was then measured using FITC-Dextran as described in the Methods. **B.** GSDC control or YKL-40 shRNA cells were used for the same permeability assay **(Top)** as described in **(A)**, in the presence of an anti-N-cad Ab (50 μg/ml) **(Middle)** or VEGF Ab (100 ng/ml) **(Bottom)**. **C.** GSDC control or YKL-40 shRNA cells were first plated on the insert. 2 hr following attaching and spreading, HMVECs were plated on the top of the GSDCs to form a second layer and allowed to attach and spread in the presence of mIgG or an anti-VEGF Ab (100 ng/ml). The same permeability assay was performed on the next day. **D.** GSDCs were pre-treated with mIgG or an anti-N-cad Ab (50 μg/ml) overnight to exclude the possibility that the top layer of HMVECs prevents the antibody from access to the bottom layer of GSDCs. Then, GSDCs and HMVECs were set up as described in C in the presence of mIgG or an anti-VE-cad Ab (20 μg/ml). The permeability was measured. N=6, *P≤0.05 compared to corresponding controls at the same time points.

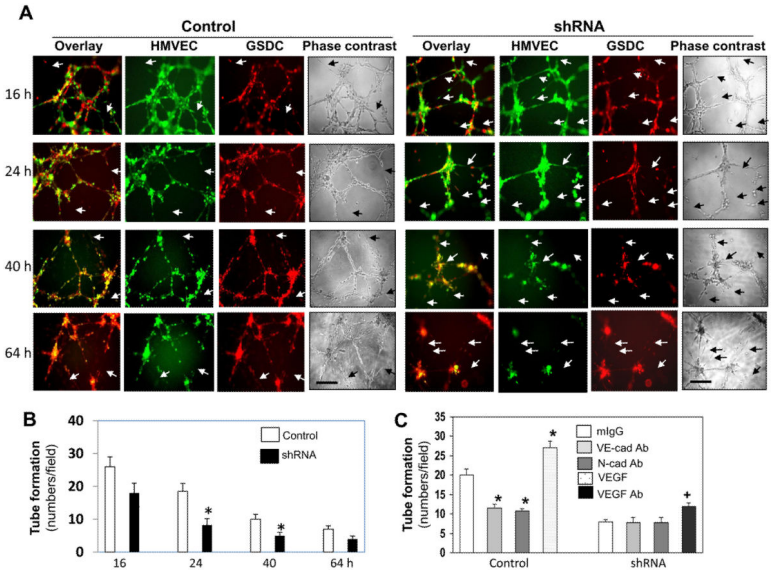

Figure 7. GSDCs expressing YKL-40 stabilize endothelial cell vessels in a manner dependent on VE-cadherin and N-cadherin activity

A. HMVECs and either control or YKL-40 shRNA GSDCs were pre-stained with Calcein AM (green) and Calcein red, respectively, and plated together on Matrigel. Tube formation was analyzed over a 64-hour time course and representative images were shown at 16, 24, 40, and 64 hr. White arrows demonstrated breaks in the tube networks, while black arrows on the phase contrast images depicted gaps in the corresponding networks. Bars: 100 μm. **B.** Quantification of the tubules formed by HMVECs plus control or YKL-40 shRNA GSDCs. N=3, *P≤0.05 compared to controls. **C.** Same condition as described in A was set up in the presence of recombinant VEGF (10 ng/ml), an anti-VEGF (100 ng/ml), VE-cadherin (20 μg/ml), or N-cadherin antibody (50 μg/ml). 24 hr following incubation, tubules with fluorescence were analyzed and quantified. N=3, *P≤0.05 compared to mIgG.

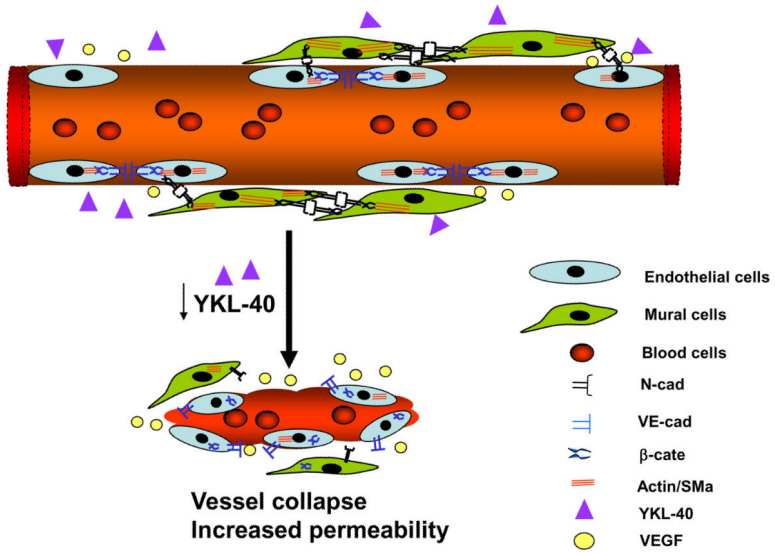

Figure 8. A hypothetical model of vessel stability and angiogenesis mediated by YKL-40-expressing mural cells

A tumor blood vessel is covered with mural cells that express high YKL-40 levels. YKL-40 promotes cell-cell contacts of mural cells via enhanced N-cadherin/β-catenin interaction and downstream effector SMa in an autocrine manner. In addition, YKL-40 also induces VE-cadherin/β-catenin/actin association in endothelial cells in a paracrine loop. Once expression of YKL-40 is inhibited, both mural cell and endothelial cell contacts are disrupted, which impairs vascular permeability and stability. As a result, the diminished angiogenesis restricts nutrients and oxygen delivery to the tumors, impeding the tumor growth.